

**REPORT DOCUMENTATION PAGE**Form Approved  
OMB No. 0704-0188

Public reporting burden for this collection of information is estimated to average 1 hour per response, including the time for reviewing instructions, searching existing data sources, gathering and maintaining the data needed, and completing and reviewing this collection of information. Send comments regarding this burden estimate or any other aspect of this collection of information, including suggestions for reducing this burden to Department of Defense, Washington Headquarters Services, Directorate for Information Operations and Reports (0704-0188), 1215 Jefferson Davis Highway, Suite 1204, Arlington, VA 22202-4302. Respondents should be aware that notwithstanding any other provision of law, no person shall be subject to any penalty for failing to comply with a collection of information if it does not display a currently valid OMB control number. PLEASE DO NOT RETURN YOUR FORM TO THE ABOVE ADDRESS.

**1. REPORT DATE (DD-MM-YYYY)**

29-08-2002

**2. REPORT TYPE**

Final

**3. DATES COVERED (From - To)**

01/2001 - 07-2002

**4. TITLE AND SUBTITLE**

Evaluation of Residual Stresses and their Influence on  
Distortion in the De-coiling and Welding Processes

**5a. CONTRACT NUMBER****5b. GRANT NUMBER**

N00014-00-1-0807

**5c. PROGRAM ELEMENT NUMBER****5d. PROJECT NUMBER****5e. TASK NUMBER****5f. WORK UNIT NUMBER****6. AUTHOR(S)**

Wojciech Z. Misiolek  
Pawel Kazanowski

**7. PERFORMING ORGANIZATION NAME(S) AND ADDRESS(ES)**

Institute for Metal Forming  
Lehigh University  
5 East Packer Ave.  
Bethlehem, PA 18015

**8. PERFORMING ORGANIZATION REPORT NUMBER****9. SPONSORING / MONITORING AGENCY NAME(S) AND ADDRESS(ES)**

Office of Naval Research

**10. SPONSOR/MONITOR'S ACRONYM(S)**

ONR

**11. SPONSOR/MONITOR'S REPORT NUMBER(S)****12. DISTRIBUTION / AVAILABILITY STATEMENT**

Approved for Public Release, distribution is Unlimited

**20030402 049****13. SUPPLEMENTARY NOTES**

N/A

**14. ABSTRACT**

An analysis of de-coiling process is provided. The expression for equilibrium of internal stresses within de-coiled plate during welding was established. First simulations of the de-coiling process have been prepared using Finite Element Modeling technique. Experimental verification of numerical results has been performed. The experimental results are in very good agreement with the numerical results. More insight into the changes of the sample material during deformation was achieved by careful microstructural examination. The microhardness measurements were proposed as a new and fast method of indicating the position of the neutral plane within de-coiled plate. Based on literature review and results of performed analysis a set of general rules for assembling a large structure by welding from de-coiled plates was proposed. Based on that set it will be possible to predict de-coiled plate distortion during welding.

**15. SUBJECT TERMS****16. SECURITY CLASSIFICATION OF:**

a. REPORT

b. ABSTRACT

c. THIS PAGE

**17. LIMITATION OF ABSTRACT****18. NUMBER OF PAGES**

33

**19a. NAME OF RESPONSIBLE PERSON**

Wojciech Z. Misiolek

**19b. TELEPHONE NUMBER (include area code)**

(610) 758 - 4252



# **Evaluation of Residual Stresses and their Influence on Distortion in the De-coiling and Welding Processes**

**Office of Naval Research  
Final Report**

**Pawel Kazanowski and Wojciech Z. Misiolek**

**Institute for Metal Forming at Lehigh University  
Bethlehem, PA**

**DISTRIBUTION STATEMENT A**  
Approved for Public Release  
Distribution Unlimited

**August 2002**

## **Technical Objectives**

- Executive summary
- Introduction
- Stages in the construction of a physical model

## Executive summary

The objective of the project is to develop a model capable of predicting the springback effect in de-coiled plates prepared for the welding processes in order to fabricate high precision guideway beam system for the magnetic levitated trains. Collaboration between the engineering personnel of the USX (US Steel Group), Maglev and the Institute for Metal Forming (IMF) at Lehigh University is envisioned for the future stages of the project. This collaboration ensures exchange of research ideas, access to the experimental material and material physical data necessary for performing designed physical and numerical experiments. Upon completion, the performed research will allow the selection of the optimal thermo-mechanical treatments to guarantee the most uniform stress distribution with the neutral axis in the mid-thickness of the plate. These findings are critical in order to optimize the cross section uniformity of the uncoiled plate, which is then welded into a guideway beam where the dimensional tolerances are extremely critical.

An analysis of bending and de-coiling process is provided. First simulations of the de-coiling process have been prepared using Finite Element modeling technique. In the next six months research will be focus on the development of the material model for numerical simulation. A continuation project involving experimental verification of the numerical results is proposed.

## Introduction

It is critical that the guideway beam system for the magnetic levitated train is built with the highest precision. One of the cost reduction procedures proposed in this fabrication process is utilization of the coiled plates. The main general project objective as described in the Maglev Proposal *is full automation and integration of various manufacturing processes*. Therefore, it is necessary not only to analyze and understand the plate's springback during uncoiling but also the origin of the residual stresses responsible for plate distortion. Our goal is to develop a model, which can describe

influence of different processing parameters and material characteristics on plate distortion (see Fig.1). Distribution of residual stresses in uncoiled plate is not uniform and needs to be understood and quantitatively described. The plates are coiled immediately after hot rolling and therefore are free of residual stresses or the level of the residual stresses is very low. However, the plate material after de-coiling is not ready for further processing like welding due to presence of the residual stresses. It is necessary to straighten and flatten the plate, which after de-coiling in room temperature has built-in residual stresses. These stresses are not uniformly distributed in the uncoiled plate making straightening and flattening very challenging. It is very important to understand how the de-coiling parameters and coil characteristics are influencing the presence of the residual stresses and their distribution. It is crucial to understand the influence of every simple parameter, which can contribute to deficiencies in beam flatness, straightness, and dimension accuracy.

There are two potential solutions to the distortion problem. One requires localized heating and has been developed by Air Products Company. The second one is based on mechanical straightening and required hardware can be custom built for de-coiling application. A thermo-mechanical model can provide understanding of the origins of the distortions and be used in application in one of the two, above mentioned techniques.

### **Constructing the physical model**

Flow chart illustrating the stages in the construction of a physical model is presented on Figure 1 after M.F. Ashby [1]. The first stage consists of an identification of the problem and a consideration of the likely physical mechanisms involved. A model should be constructed using the most advanced theory available and after making a thorough assessment of the published literature. This usually identifies areas where adequate knowledge does not exist, in which case approximations must be made in order to achieve progress. The lack of theory or material and process data can spark a new research as resources become available, but need not unduly hinder the formulation of a model. In practice, this means that the targeted precision has to be chosen to suit the state of the art in the studied subject.

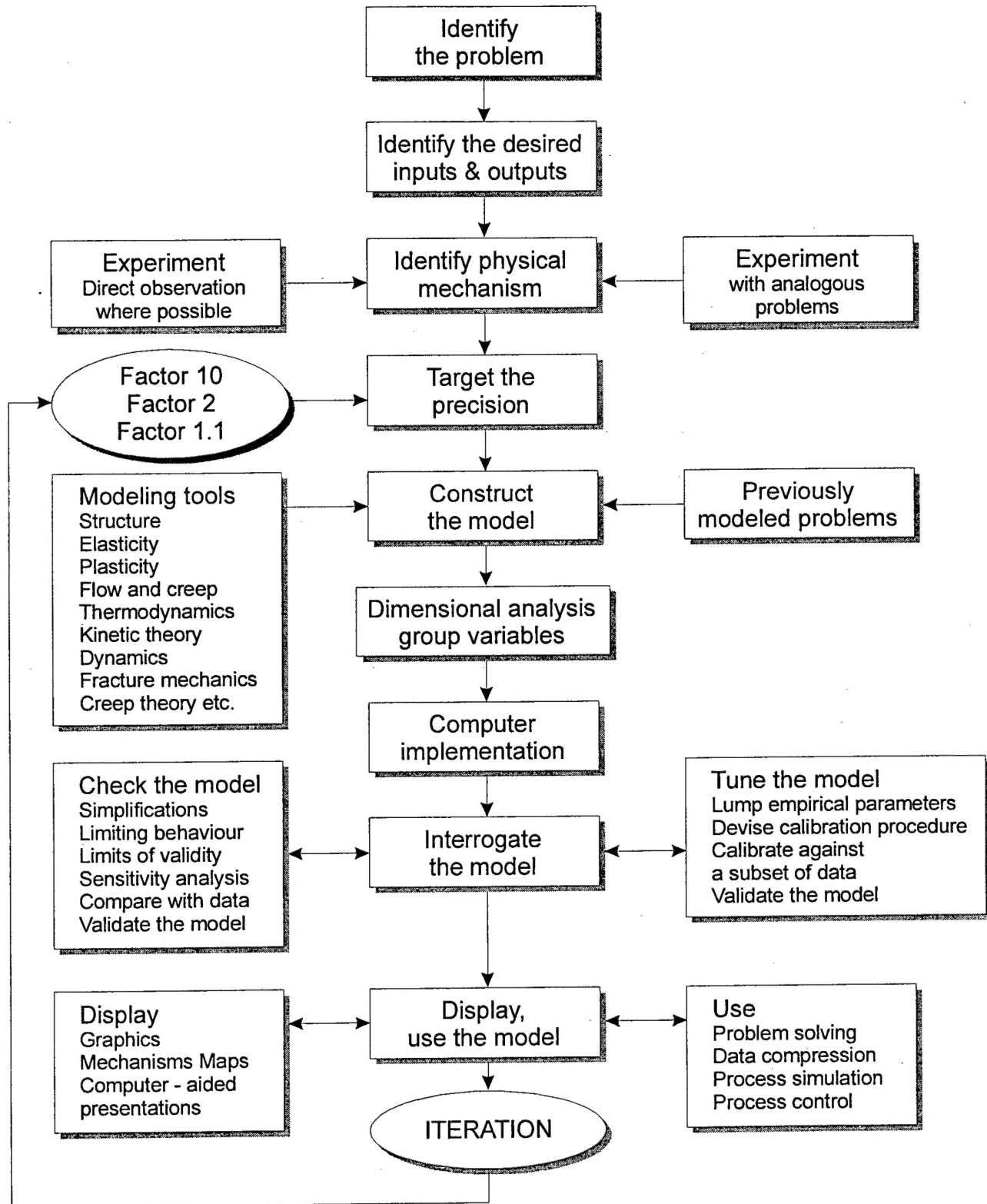


Fig. 1. Flow-chart illustrating the stages in the construction of a physical model. At each stage, iteration back to the earlier stages may be required.[1]

## **Technical Approach**

- Problem definition
- Guideway overview
- Guideway Beam materials description
- The proposed studies
- List of the main objectives of each project phase
- Summary of work accomplished during 2001

## Problem definition – Guideway overview

The Transrapid guideway is an integral component of the Transrapid Maglev System. Consisting of high-precision welded steel or reinforced concrete columns and foundations (substructures), the overall system ride comfort is directly related to the execution and quality of the guideway. Therefore, guideway specifications and tolerances that relate to ride comfort are especially important [2]. In order to develop a model capable of predicting the springback effect in de-coiled plates prepared for the welding it is necessary to gather physical data related to such process parameters and material characteristic as:

- Coil size
- Coil thickness
- Coiling temperature
- Selected steel grade
- Flow stress and ultimate strength data, etc.

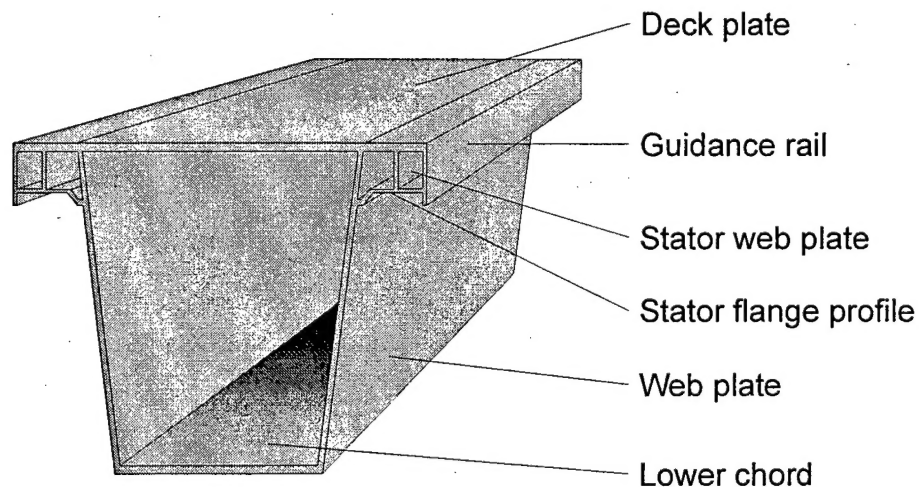


Fig. 2. Schematic view of the steel guideway beam.[2]



The steel guideway, (see Figure 2), is comprised of individual trapezoidal box girders (beams) with cantilevered side guide rails and stator packs, which are attached to the stator-pack flange underneath each cantilevered side of the beam deck. Bolts attach the stator packs to the flange. Bearings are attached with anchor bolts, anchor rods, or shear studs to the concrete substructure supporting the beams, [2]. Hot rolling and coiling of plates at elevated temperatures, (see Figure 3), with the de-coiling in room temperature before welding is one of the recommendations for potential cost saving strategies.

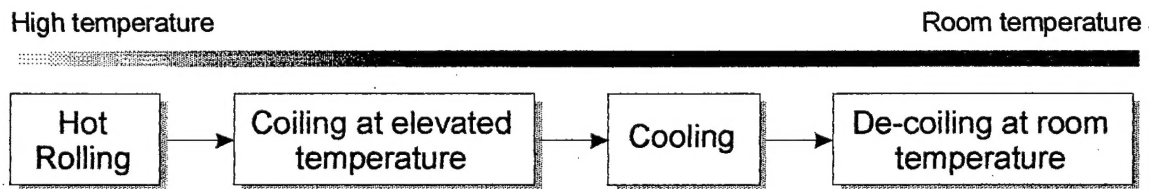


Fig. 3. Order of operations with approximate temperature level.

As mentioned before the distribution of residual stresses within each guideway steel component is uneven. The outside layers of material are exposed to higher strain while inside coil material, in the eye of the coil, is experiencing much lower levels of the compression strains. The distribution of residual stresses is function of above mentioned parameters and will effect mechanical properties of the plate after de-coiling. Since residual stresses are not uniform in such situation the neutral axis will not be positioned in the mid-thickness of the plate and it will be shifted to a new location dictated by the parameters of the coiling and de-coiling process.

The steel guideway beam is fully welded with integrated functional components, lateral guidance rails, and gliding plane. The design of the steel beam largely takes into account automated manufacturing processes. The concrete guideway beam is a pre-stressed, post-tensioned, reinforced concrete structure with integrated lateral guidance rails, and gliding plane. Attached to the steel or concrete beams, is the guideway equipment, which includes the long-stator packs, cable windings, power rails for vehicle battery charging, and various bolted-on connections.

## Guideway Beam materials

The steel used in the guideway beams, their properties presented in Table 1, and their semi-finished product dimensions are compiled in this section. All length units – if not stated otherwise, are in millimeters [mm]. A schematic overview of the guideway beam is shown in Figure 2.

Tab. 1. Mechanical properties for Guideway plate materials

|                           | RSt 37-2 <sup>1</sup> | St 52-3 <sup>2</sup> | MSH Steel <sup>3</sup> | Unit                | Remarks             |
|---------------------------|-----------------------|----------------------|------------------------|---------------------|---------------------|
| <b>R<sub>eH min</sub></b> | 225                   | 345                  | 360                    | N / mm <sup>2</sup> | Yield point         |
| <b>R<sub>m</sub></b>      | 340 – 470             | 490 – 630            | 510                    | N / mm <sup>2</sup> | Tensile strength    |
| <b>A<sub>5 min</sub></b>  | 26                    | 16                   | 36                     | %                   | Elongation at break |
| <b>A<sub>V min</sub></b>  | 27                    | 27                   | 12                     | J                   | Impact strength     |

<sup>1</sup> structural carbon steel, ASTM A 283-78

<sup>2</sup> structural HSLA (high-strength, low-alloy) steel, ASTM 440-77

<sup>3</sup> steel with high electrical resistance that results in a considerably low magnetic drag due to the eddy currents

Tab. 2. Chemical composition (Hot Metal Analysis) for Guideway plate materials

| Elements      | RSt 37-2  | St 52-3 | Unit |
|---------------|-----------|---------|------|
| <b>C</b>      | ≤ 0.200   | 0.230   | %    |
| <b>Mn</b>     | 0 – 1.500 | 1.700   | %    |
| <b>P</b>      | 0.050     | 0.045   | %    |
| <b>S</b>      | 0.035     | 0.045   | %    |
| <b>Others</b> | 0.009     | -       | %    |

### Semi-finished Parts (Wrought Dimensions) - Requirements

The material dimensions shown in the following Table are given for the Type I beams since these beams are the largest and therefore have the largest material requirements (the worst case scenario).

Tab. 3. Plate Requirements for German Project, Type I Guideway Beams

| Utilized for          | Wrought-Dimensions<br>(L x W x t)                                    | Tolerances Typically:   |
|-----------------------|--|---|
| Deck Plate            | 21000 x 3000 x 18  | according to EN 10029;<br>Class "S"<br>Extra Requirement:<br>$e = 0,5 \times 3 = 1,5$ [mm/m]<br>(e= flatness) |
| Webs                  | 21000 x 2050 x 12  | according to EN 10029;<br>Class "S"   |
| Lower Chord           | 21000 x 870 x 40 or<br>21000 x 1720 x 40 or<br>21000 x 2560 x 40 (*) | according to EN 10029;<br>Class "S"   |
| Stator Web Plate      | 21000 x 210 x 15 or<br>21000 x (nx210) x 15 (*)                      | according to EN 10029;<br>Class "S"   |
| Stator Flange Profile | 21000 x 320 x 71,4   | Special Rolled Section  |
| Guidance Rails        | 21000 x 310 x 30 or<br>(21000 x (nx310) x 30) (*)                    | according to EN 10029;<br>Class "S"<br>Extra Requirement:<br>$e = 0,5 \times 3 = 1,5$ [mm/m]<br>(e= flatness) |

(\*): Dimensions are approximate values. Final precision measurements of the semi-finished products (sheet metal parts) depend on the manufacturing conditions (overlapping, burner facility and transportation) of the given manufacturer.

The proposed studies, presented in Figure 4, are generally divided into three Phases with the main objectives listed for each Phase as follows:

- Phase I: **Evaluation, measurements and calculations of the physical data responsible for the residual stresses during de-coiling. Steel selection. Microstructural characterization.**
- Phase II: **Development of the springback model as a function of residual stresses for the de-coiling operation.**
- Phase III: **Testing and verification of the model for different process conditions and material characteristic.**

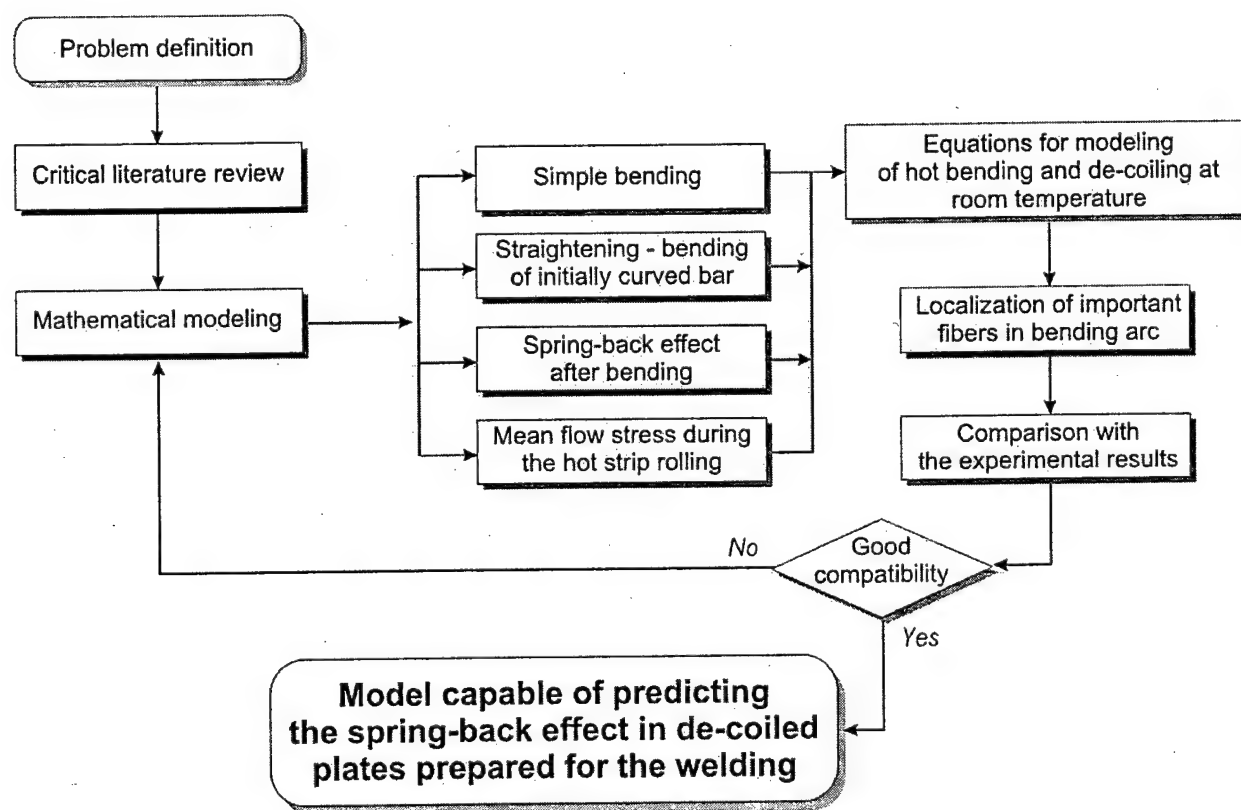


Fig. 4. Flow chart for performed studies. At each stage, iteration back to the earlier stages may be required.

### Summary of work accomplished during 2001

Based on the literature review [1-12] and theory of bending it becomes obvious that during developing a model capable of predicting the spring back effect in de-coiled plates we have to consider several process parameters. Among them two are of critical importance. First is the influence of initial curvature radius on stress distribution during bending and second the ration between width and thickness of the curved plate.

As shown previously, a plate has tendency to bulge during bending. Based on the literature review one can say, that the tendency for bulging is increasing with decreasing width of plate for the same thickness. The steel guideway, (see Figure 2), is fully welded with integrated functional components, lateral guidance rails, and gliding plane. Table 4 consists of the results of calculations for bulging tendency for few components of steel guideway.

Tab. 4. Tendency for bulging calculated from wrought dimensions  
for steel guideway elements

| Steel Guideway element | Wrought-Dimensions (L x W x t)                | W / t factor | Bulging tendency |
|------------------------|---|--------------|------------------|
| Deck Plate             | 21000 x 3000 x 18                             | 166          | very low         |
| Webs                   | 21000 x 2050 x 12                             | 170          | very low         |
| Lower Chord            | 21000 x 870 x 40 or                           | 21           | high             |
|                        | 21000 x 1720 x 40 or                          | 43           | medium           |
|                        | 21000 x 2560 x 40 (*)                         | 64           | medium           |
| Stator Web Plate       | 21000 x 210 x 15 or<br>21000 x (nx210) x 15   | 14           | high             |
| Stator Flange Profile  | 21000 x 320 x 71,4                            | 4            | very high        |
| Guidance Rails         | 21000 x 310 x 30 or<br>(21000 x (nx310) x 30) | 10           | very high        |

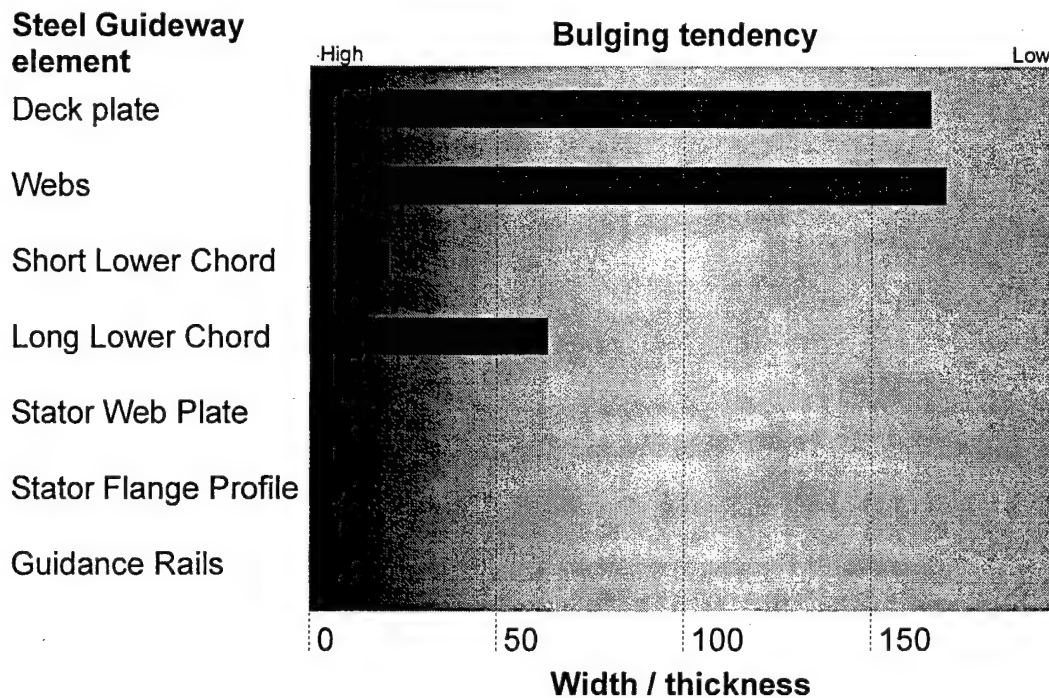


Fig. 5. Tendency for bulging calculated from wrought dimensions for steel guideway elements

Above width to thickness ratio equal 15 the tendency for change the cross-section from rectangular onto trapezoid is medium and with increase of this ratio is decreasing. In Figure 5 results from Table 4 are presented. Short Lower Chord, Stator Web Plate, Guidance Rails and especially Stator Flange profile are those elements of steel guideway, which are going to bulge during de-coiling. One of the methods of avoiding is producing straight profiles. But, cost saving strategy suggest producing coiled elements much easier to transport. Calculations for optimal inner coil radius are also very important. The tendency for surface cracking is increasing with decreasing of the inner curvature radius. Based on performed calculations became clear, that above the ratio between initial height of section  $h$  and initial radius of curvature  $a$ , equal or high  $1/15$  the bending stress on the convex surface decrease. Also, the distance  $e$ , between center-of-gravity and neutral axes decreases and stays almost on the same level. This tendency is present for rectangular and trapezoid cross-section.

### Calculations for Residual Stress level and distribution

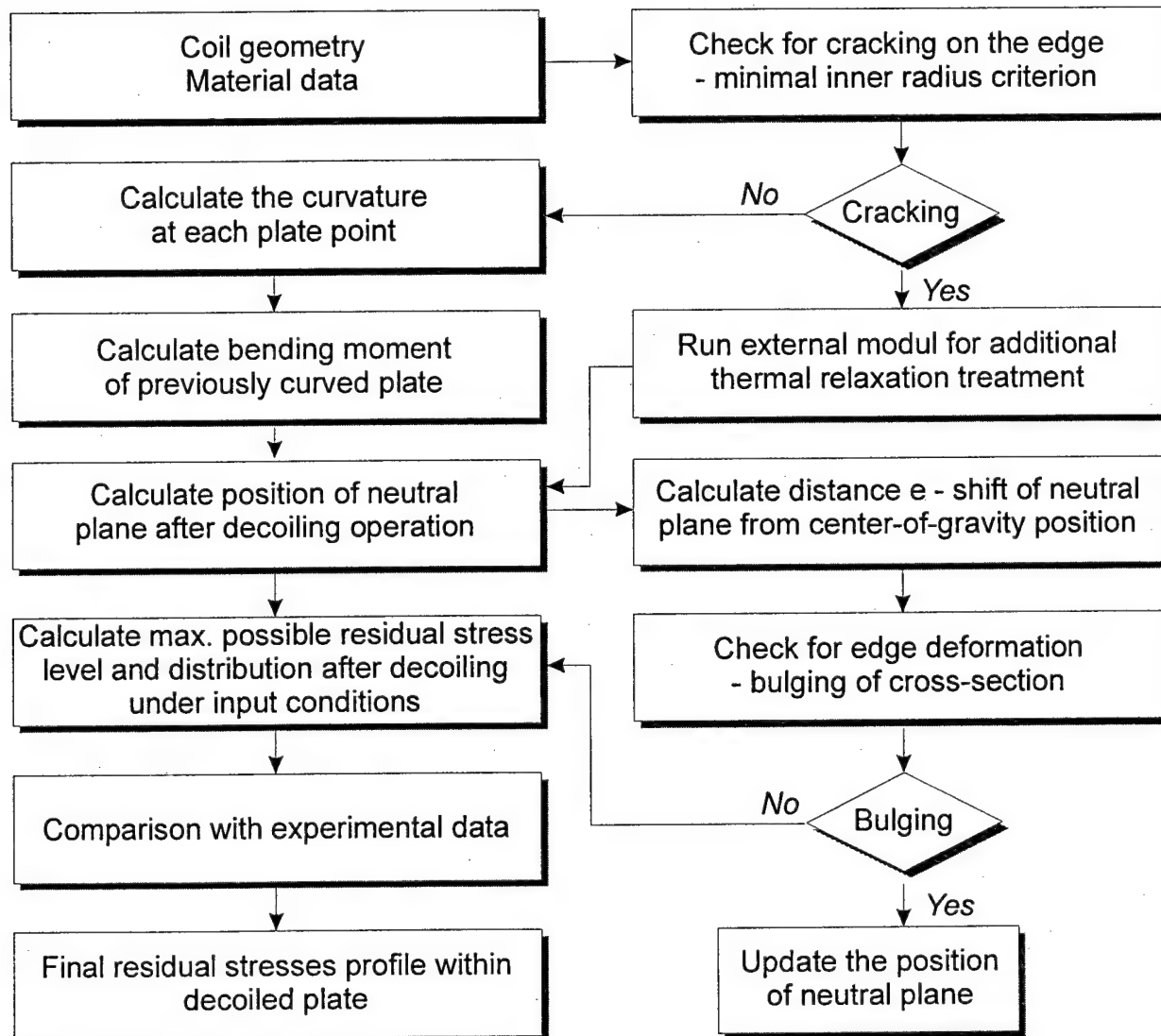


Fig. 6. Algorithm for calculations of final residual stresses profile within previously curved plate with implementation of cracking and bulging criteria.

Essential parts of algorithm for calculations of final residual stresses profile within previously curved plate are cracking and bulging criteria. Basis calculations of initial curvature as a function of plate length are the first part of computer code presented in Figure 6. From the input data describing the coil and its material, one can predict the

cracking possibility during straightening. Proposed criterion is based on theory of bending and includes data for material behavior during plastic deformation. In case of positive response in terms of cracking the outer module for thermal treatment conditions will be activated. Second stage of proposed code is checking for cross-section deformation during de-coiling operation. As shown previously, the influence of cross-section shape on the shift of neutral plane from center-of-gravity position is different for rectangular and trapezoid cross-section. In the worse case scenario, one part of de-coiled plate will remain with rectangular cross-section and the other part will be distorted. Calculations for described deformations are possible if we consider theory of bending and proposed criterion for bulging arising from calculations for neutral plane placement. It is also possible to calculate the distortion only within a part of plate.

Using data from the first and second stage description of residual stress level become possible. As boundary conditions, we are assuming that the maximum level of residual stresses is equal to stress level calculated in previous step. The real stress level within plate is a function of many variables. Among them, the most important is behavior of material during deformation. It is planned to propose follow-up studies to the current modeling research. The objective of the follow-up project will be to provide experimental verification of the FEM results. For the modeling purposes the material constitutive equations from the theory of plasticity will be used.

The last part of described code is a module for comparison calculated data with experimental results. Two experimental methods: microhardness measurements and strain gage measurements have been selected.



## **Progress**

- Mathematical Analysis
- Recent results and their discussion
  - FEM modeling
  - Experimental verification
  - Micro-Structural aspects
- Summary - Guidelines for the de-coiling technology
- Meetings and presentations
- References

## Mathematical Analysis

### *Definition of a Mathematical Model*

A mathematical model generally consists of algebraic or differential equations, which quantitatively represent a system or process. For example, it may be a relationship that defines the time to solidify an ingot, the stress distribution in a forging die, the processing conditions needed to obtain given microstructure, and so on. Mathematical models provide a fundamentally based quantitative relationship between process variables. Mathematical models are helpful for providing a general insight into the overall behavior of a given system. More specifically, for a new process a mathematical model will provide a guidance regarding general feasibility such as the consistency of a novel process concept with the physical and particular laws. If the process concept is judged feasible, the model may identify critical areas that will require further, possibly experimental work. [13]

A key function of a mathematical model in the study, both existing and new process, is to provide the means for the planning of experimental programs, and for the interpretation of the obtained results. [14]

### *Problem formulation*

The main objective of the proposed mathematical modeling is to find the relationship describing the evaluation of residual stresses and their influence on distortion in the de-coiling and welding processes. Residual stress is usually defined as the stress that remains in mechanical parts that are not subjected to any outside stresses. It is a result of the metallurgical and mechanical history of each point in the part and the part as a whole during its manufacture.

When a part is subjected to a field of elastic residual stresses characterized by a tensor  $\sigma_R$ , on which is superposed a field of service stress defined by tensor  $\sigma_S$ , the real stress to which the part is subjected is characterized by the tensor  $\sigma_R + \sigma_S$  (see Figure 7)

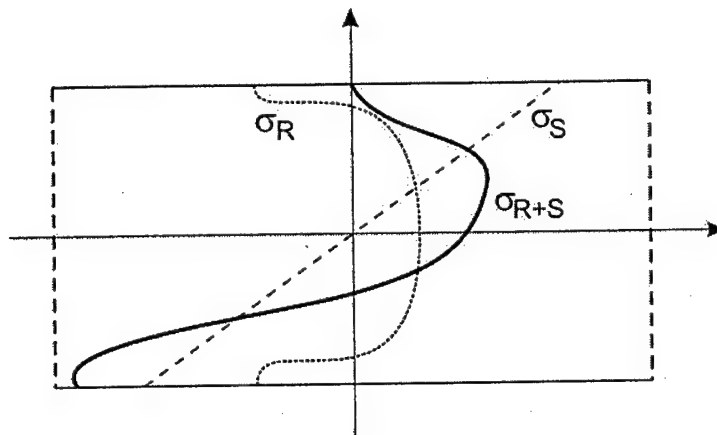


Fig. 7. Superposing of residual stresses and service stresses [15]

Relaxation of residual stresses in the real case occurs by complex interaction of a large number of factors. It depends not on the residual stress state itself but also on the material state, loading conditions, geometry, and environment of the component under consideration.

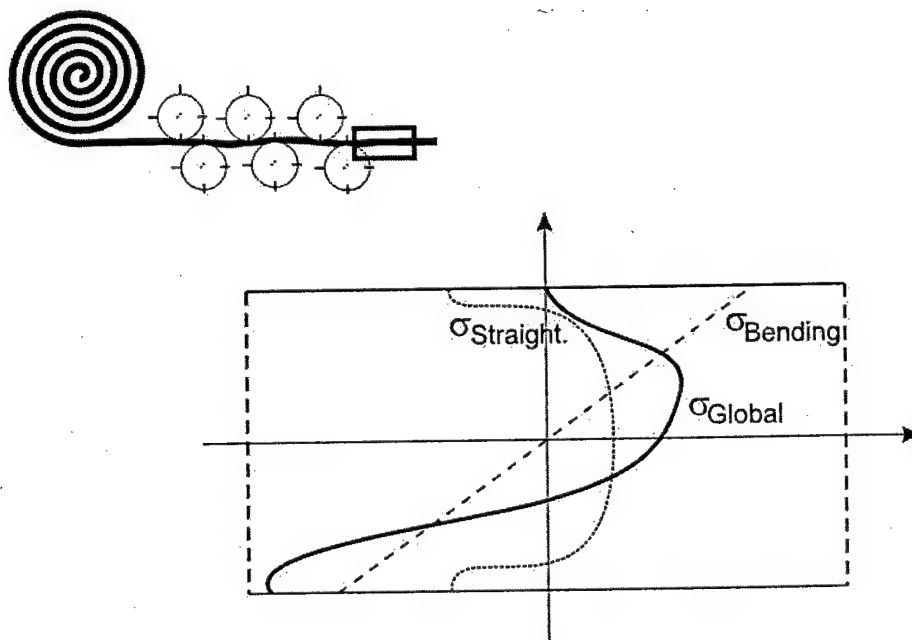


Fig. 8. Superposing of the global residual stresses ( $\sigma_{Global}$ ) within a plate as a result of simultaneous straightening ( $\sigma_{Straight.}$ ) and bending ( $\sigma_{Bending}$ ).

In Figure 8 one of possible superposing of the global residual stresses ( $\sigma_{\text{Global}}$ ) within a plate as a result of simultaneous straightening ( $\sigma_{\text{Straight.}}$ ) and bending ( $\sigma_{\text{Bending}}$ ) is presented. According to the residual stresses definition, processing residual stresses are present inside the component even if the outside constraints are not present. Any action from the outside of the component may alter the existing equilibrium of stresses and the change in the component geometry will occur. A vertical displacement  $\delta$  (see Figure 9), of the free-end of an uncoiled low carbon steel plate during welding may be predicted and control based on the following equation:

$$\delta = \frac{q \cdot x^2}{24 \cdot E \cdot I} \quad (1)$$

where

$\delta$  – vertical displacement

$q$  – complex loading conditions as a result of (i) continuous load from plate weight and (ii) non-uniform distribution of residual and thermal stresses

$x$  – length of the plate subjected to bending

$E$  – modulus of elasticity

$I$  – moment of inertia as a function of cross-section geometry

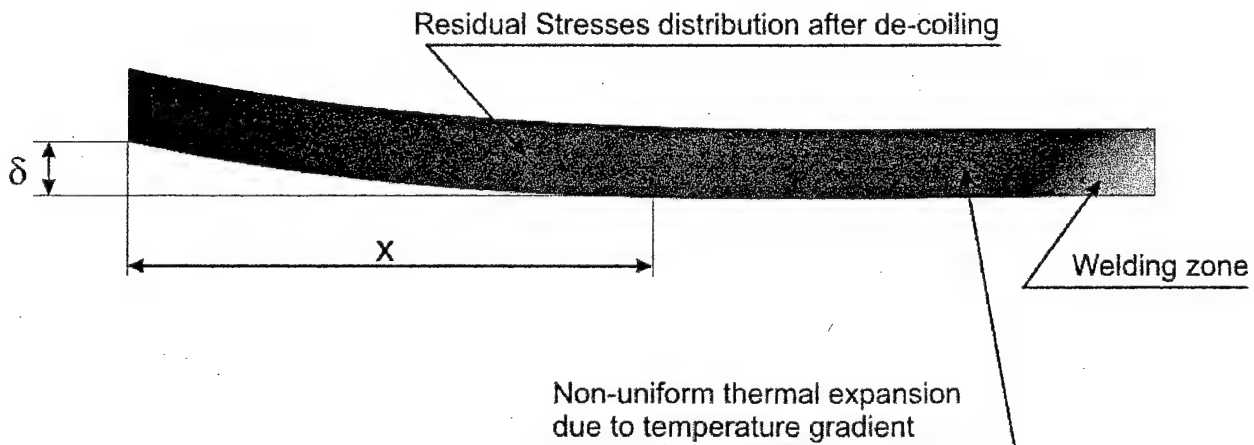


Fig. 9. Vertical displacement  $\delta$  as a result of interaction between residual stresses distribution after de-coiling and non-uniform thermal stresses due to temperature gradient during welding.

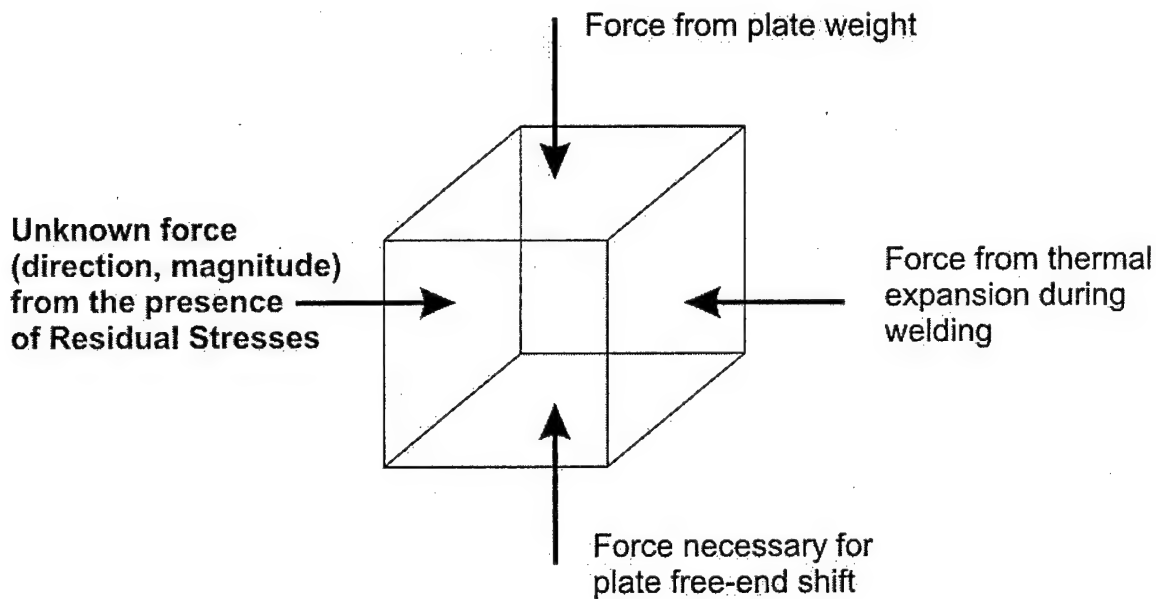


Fig. 10. Forces acting on the infinitesimal element of the plate subjected to welding.

In Figure 10 forces acting on the infinitesimal element of the plate subjected to welding are depicted. Based on the theory of mechanics the forces from plate weight and thermal expansion of the plate material during welding are possible to be calculated.

Equilibrium of stresses acting on the element of a plate is established:

$$\sigma_P = \sigma_T + \sigma_W \pm \sigma_{RES} \quad (2)$$

where:

$\sigma_P$  – stresses from plate free-end shift

$\sigma_T$  – thermal stresses due to welding

$\sigma_W$  – stresses from plate weight (see Table 5 for approximate weight of the Guideway elements)

$\sigma_{RES}$  – residual stresses after de-coiling; the sign of the residual stresses may vary and is a resultant of the global residual stresses ( $\sigma_{Global}$ ) within a plate as a result of simultaneous straightening ( $\sigma_{Straight.}$ ) and bending ( $\sigma_{Bending}$ ).

Tab. 5. Weight of the Guideway elements

| Utilized for          | Wrought-Dimensions<br>(L x W x t) | Weight [Tons] |
|-----------------------|-----------------------------------|---------------|
| Deck Plate            | 21000 x 3000 x 18                 | 9.072         |
| Webs                  | 21000 x 2050 x 12                 | 4.132         |
| Lower Chord           | 21000 x 870 x 40 or               | 5.846         |
|                       | 21000 x 1720 x 40 or              | 11.558        |
|                       | 21000 x 2560 x 40                 | 17.236        |
| Stator Web Plate      | 21000 x 210 x 15                  | 0.529         |
| Stator Flange Profile | 21000 x 320 x 71,4                | 3.816         |
| Guidance Rails        | 21000 x 310 x 30                  | 1.526         |

Residual stress level within a plate after de-coiling is high enough for plate free-end shift during welding. By rewriting equation (2) in terms of stresses and by substituting rewritten equation (1) into equation (2) one can write an equation for equilibrium of stresses acting within a plate:

$$\sigma_{RES} \geq E\alpha\Delta T + g\rho H + \frac{12\delta EI}{x^3} \quad (3)$$

where

$E$  – Young's Modulus

$I$  – Moment of inertia

$\alpha$  - coefficient of thermal expansion

$\Delta T$  – temperature gradient

$g$  – gravity acceleration

$\rho$  - material's density

$H$  – plate thickness

$\delta, x$  – experimental parameters

## Recent results and their discussion

### *FEM Modeling*

Design of a technological process, which yields good quality products, is tedious and expensive due to a high number of experiments. Nowadays, computer modeling is used for fast calculation and optimization of forming processes before any actual physical trial takes place. There are few professional software tools that can simulate material behavior during deformation. The DEFORM™ system (Design Environment for Forming) can be used to analyze most bulk metal forming processes, as long as the process can be modeled as plane strain or axisymmetric and is based on the rigid-viscoplastic material model FEM simulation [11].

It is very difficult to describe and calculate stresses in each part of a coil during de-coiling operation. Instead of that, we consider only a part of the coil as presented in Figure 11. Because of constant distance  $L$  between straightener rolls (see Figure 11.b) the length of samples for numerical and physical modeling must be equal:

$$l_1 = l_2 = l_3 \quad (4)$$

where

$l_i$ ,  $i = 1, 2$  and  $3$  – length of the sample (see Figure 11.a).

Also, all radii of samples curvature must obey the following rule:

$$r_1 > r_2 > r_3 \quad (5)$$

where

$r_i$ ,  $i = 1, 2$  and  $3$  – radius of the sample (see Figure 11.a).

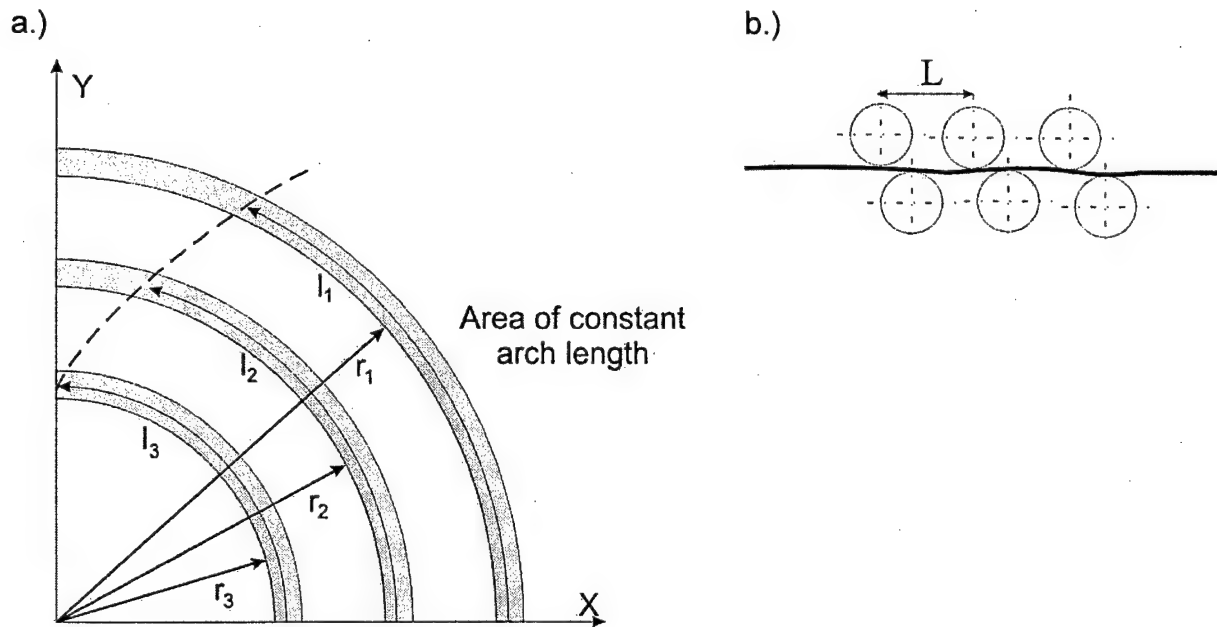


Fig. 11. Initial geometry of samples for numerical and physical modeling.  
a.) area of constant arch length, b.) constant distance  $L$  between straightener's rolls.

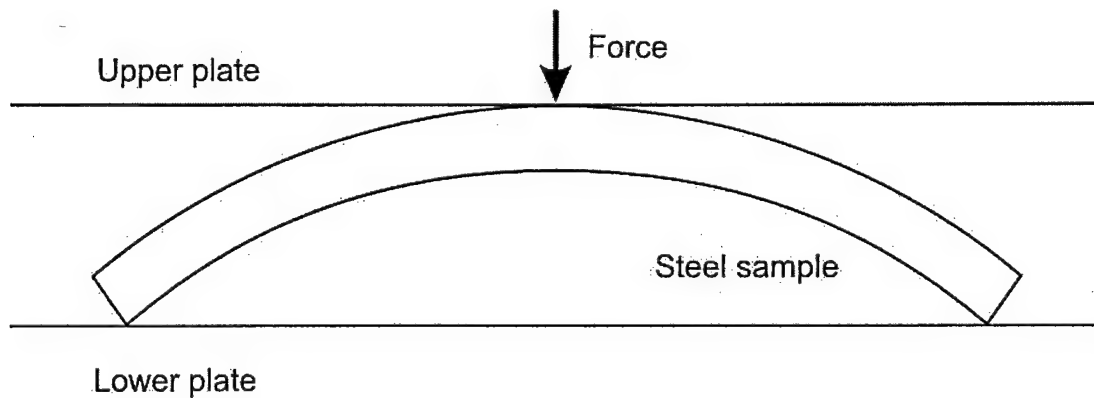


Fig. 12. Initial geometry for numerical simulation of plate bending

Numerical simulation of bending of curved plate was performed. The initial geometry for numerical simulation of plate bending is presented in Figure 12. It was assumed that the upper plate is moving vertically with the speed 0.1 in / sec. The lower plate is in the same position for the whole simulation. The calculated stroke per step was 0.01 inch. It was assumed that the steel sample material, AISI 1015 steel follows strain-stress curves during deformation.



After analysis of the effective (von Mises) stress distribution one can say, that there is a formation of neutral surface shifted from center-of-gravity line (see Figure 13). Also, it is possible to show three phases of deformation within a plate. In the very early stage the whole plate is in elastic state (see Figure 13.a), and after that, with increasing deformation the central part of the sample is entirely plastic (see Figure 13.b).

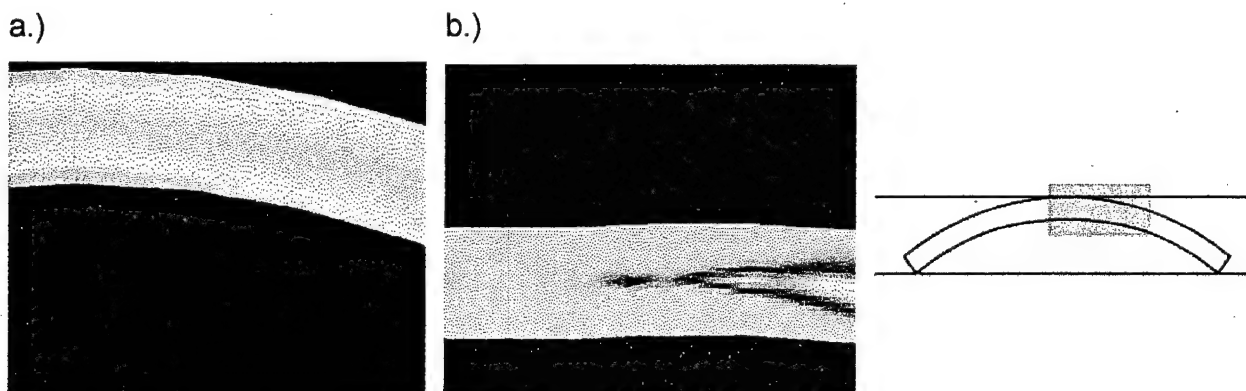


Fig. 13. Effective stress during bending the plate with initial curvature, after strokes equal 0.01 and 0.2 inch.

### *Experimental verification*

Experimental verification of the numerical results is an essential part of presented results. The steel plates with initial curvature were used. The initial radius of curvature was 2.5, 3.0 and 3.5 inch. For each radius three different sample thickness were used – 0.125, 0.250 and 0.375 inch. Length of the sample equal to 4 inch was constant for all samples used in our experiments. Compression tests were performed on INSTRON laboratory testing machine with continuous data acquisition. The results of de-coiled samples with constant thickness and different initial radius of curvature are presented in Figure 14. The upper plate stroke was identical in all cases. One can say, that with the increase in initial curvature radius from 2.5 inch to 3.5 inch the state of de-coiling expressed as a degree of sample flatterness decrease. As shown in previous report, a plate has a tendency to bulge during bending. The width to thickness ratio for samples

used in experiments was very low. Because of that fact (see Figure 5 and Table 4), the bulging tendency was very high and it was observed for all samples.

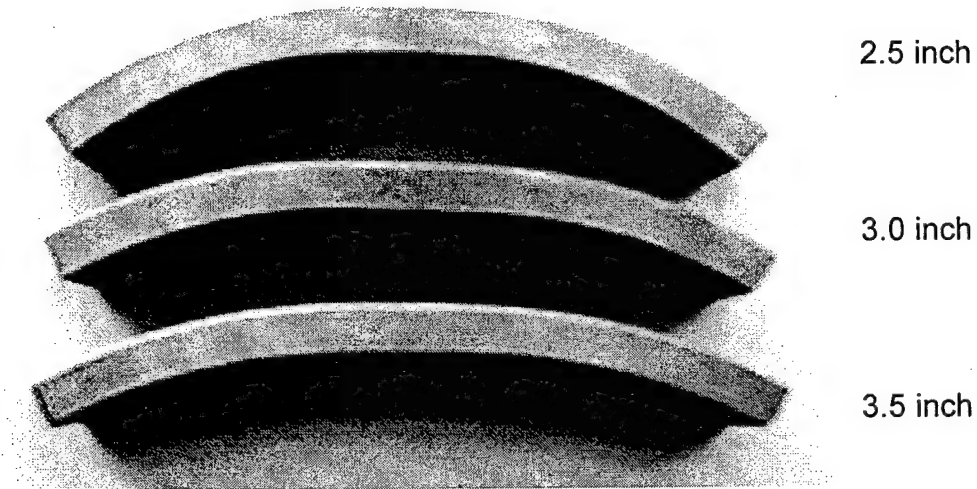


Fig. 14. Results of de-coiling samples with different radius of curvature and constant thickness.

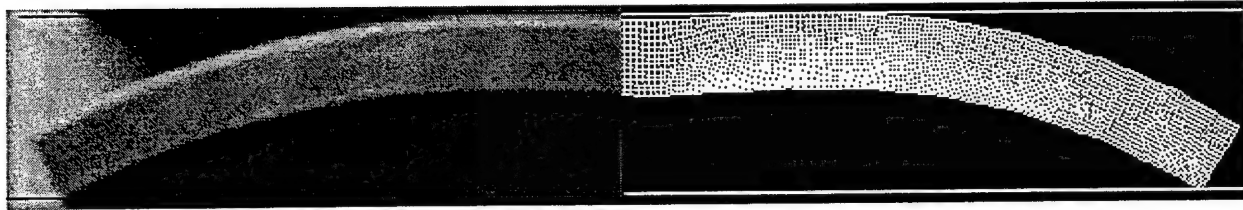


Fig. 15. Comparison between FEM (right) and Physical Modeling (left) results. The plate initial curvature radius is 2.5 inch, upper die velocity 0.1 inch / sec, and plate thickness 0.250 inch.

The change in the sample geometry during experiment was very similar to the change predicted by FEM as presented in Figure 15. Load vs. displacement curves were recorded during test. Next, they were compared to the numerical modeling results. One can say, that the curves are very similar with small difference in values (see Figure 16).

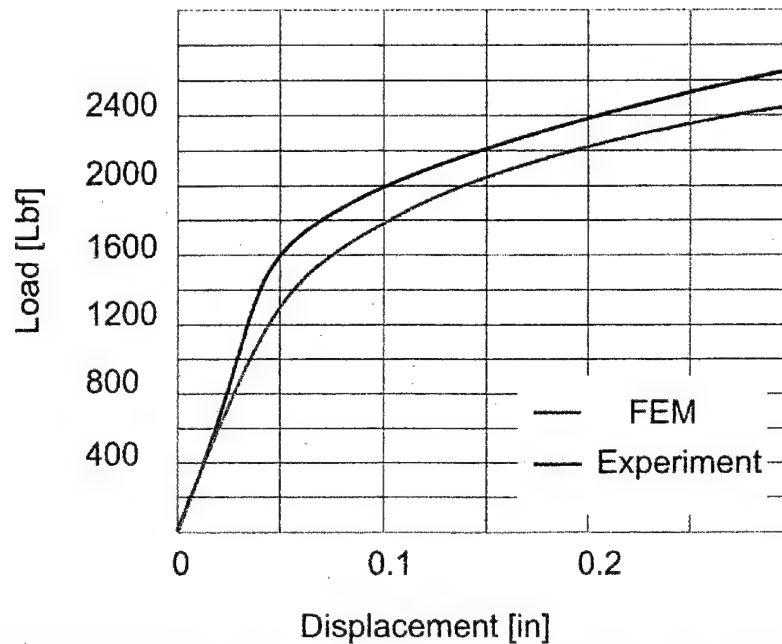


Fig. 16. Comparison between FEM and experimental results. The plate initial curvature radius is 2.5 inch, upper die velocity is 0.1 inch / sec, and plate thickness 0.250 inch.

The position of neutral plane within de-coiled plate is very important. It will influence the sign of the residual stresses component in the equation (2). After de-coiling different parts of the plate material are in different state of stresses – compressive or tensile. The correlation between microhardness and material properties such as flow stress was reported by many authors [15-17]. Hardness measurements were also used for determination of residual stresses [18]. The term microhardness usually refers to static indentation test made with loads up to 1,000 grams [19]. In our experiments the Knoop diamond indenter was used.

Measurements were performed before and after experiments. It is possible to evaluate the increase or decrease of the internal stresses based on these measurements and their analysis. The spring-back effect describes the change in shape of a formed plate upon removal from the tooling. It becomes apparent from Figure 17 that the spring-back produces enough internal stresses to alter the microhardness level. One can observe, that the microhardness distribution follows the internal stress distribution and that the neutral plane may be shifted from the geometrical center of the plate position towards inner surface of the sample.

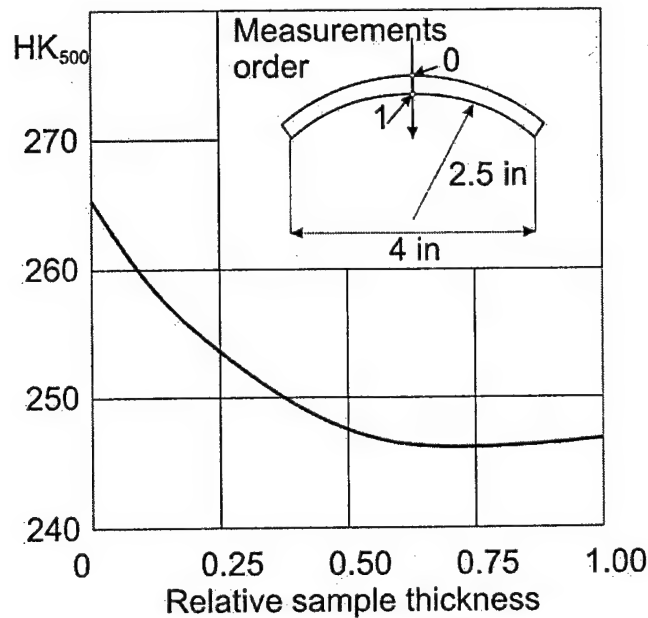


Fig. 17. Microhardness distribution across the sample thickness. Knoop indenter, load 500 grams, load time 15 sec.

#### *Micro-Structural aspects*

Residual stresses are a consequence of interactions among time, temperature, deformation, and microstructure. Material or material-related characteristics that influence the development of residual stress include:

- Thermal conductivity
- Heat capacity
- Thermal expansivity
- Elastic modulus and Poisson's ratio
- Plasticity
- Thermodynamics and kinetics of transformations
- Mechanism of transformations
- Transformation plasticity

By careful analysis of samples microstructure before and after deformation it was possible to observe some changes which are presented in the following Figures.

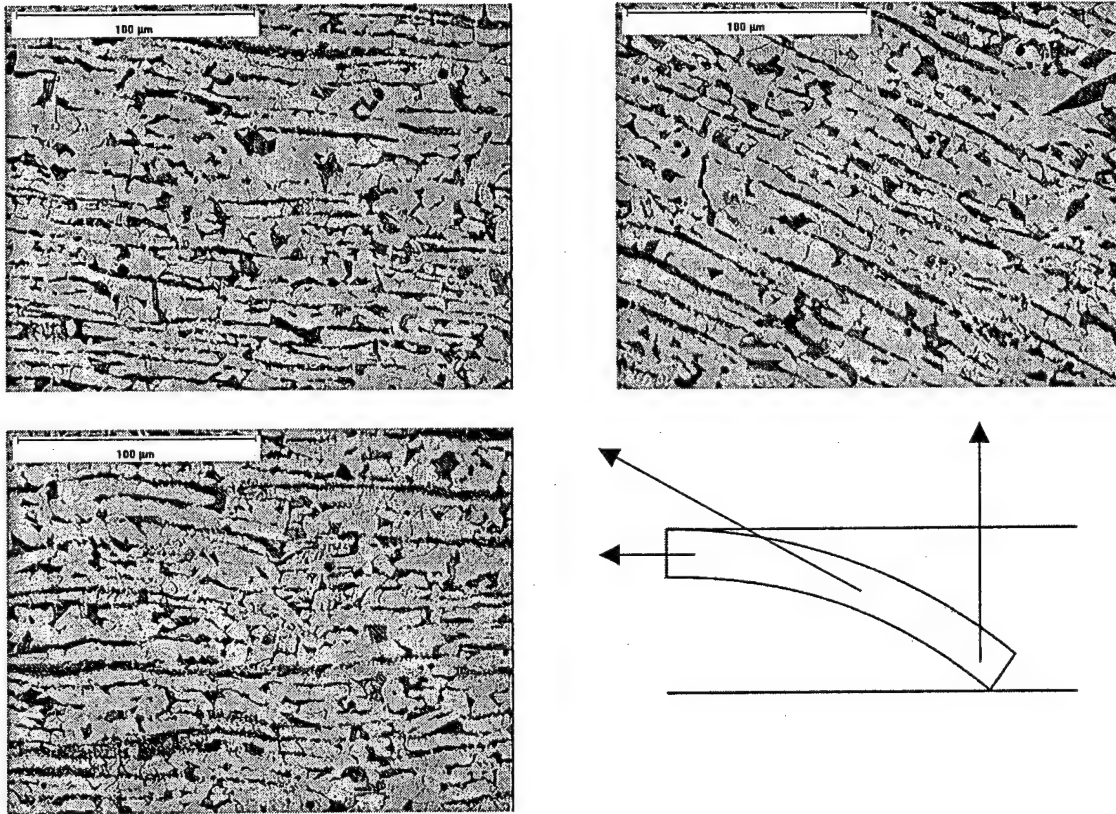


Fig. 18. Light optical micrographs of the low-carbon steel after partial de-coiling at room temperature – **neutral plane**.

In Figure 18 microstructure of steel sample after partial de-coiling is presented. One can observe that for the whole neutral plane or near it the microstructure is similar without any significant distortion. The dark phase is pearlite, the light phase is ferrite and the black precipitations are cementite. Compressive state of stress present below the top surface of the sample preserved its initial microstructure as it has been shown in Figure 19. The tensile state of stress developed near the bottom surface of the sample during de-coiling significantly alters microstructure (see Figure 19).

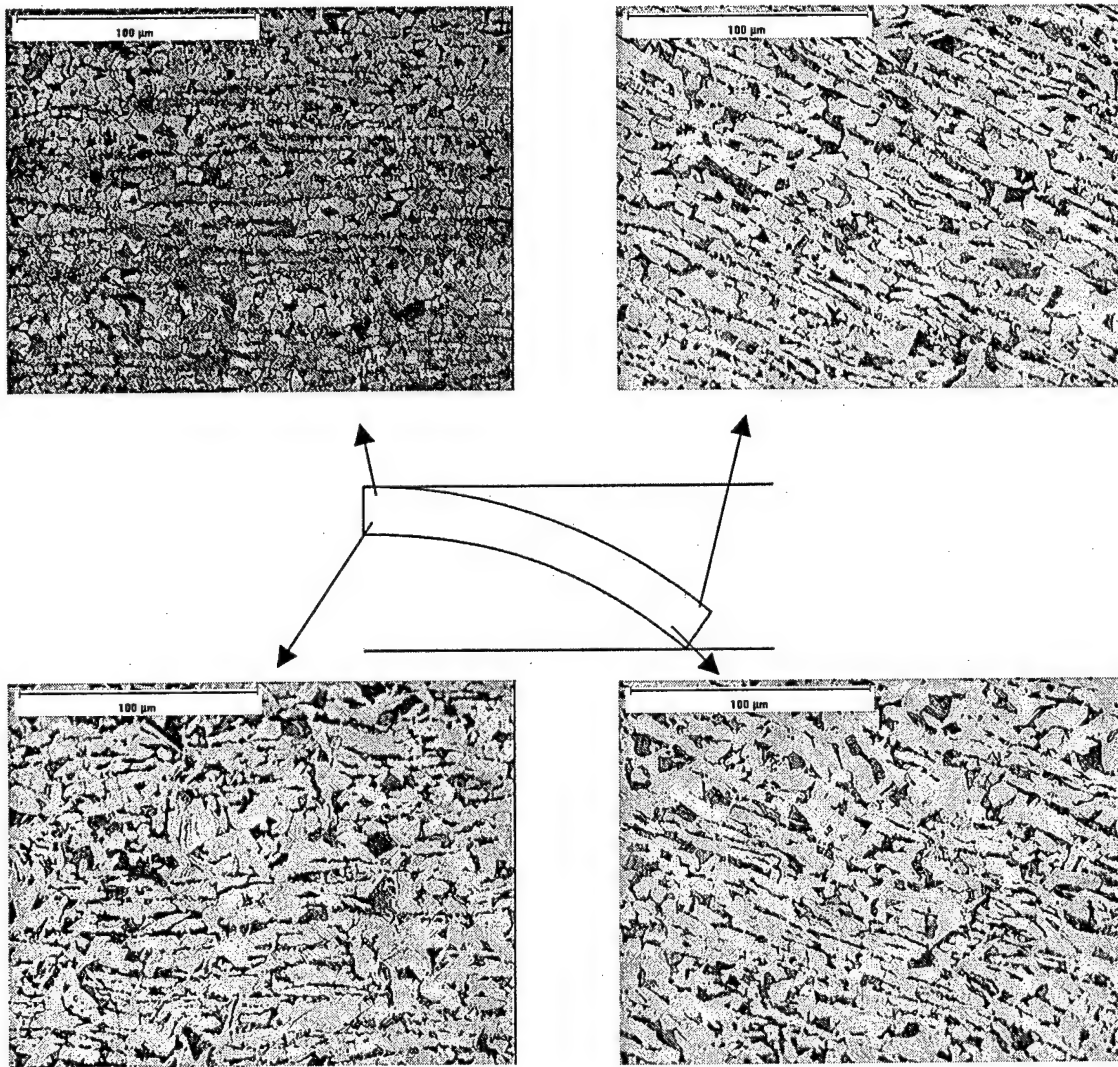


Fig. 19. Light optical micrographs of the low-carbon steel after partial de-coiling at room temperature – below top surface (top) and above bottom surface (bottom).

## **Summary - Guidelines for the de-coiling technology**

Based on the wide literature review and on the achieved experimental and numerical results it is known that the distortion during welding is dependent on de-coiling history. The equilibrium of stresses within a de-coiled plate during welding has been established in equation (3). As long as the mentioned equilibrium will be satisfied the plate will not change its shape. Two parameters  $\delta$  and  $x$  present in the equation must be evaluated experimentally.

However, from practical point of view it is not necessary to know the exact values of the stresses present within a plate. The position of neutral plane and sign of the stresses present below top surface and above bottom surface of the plate are more important. Based on that technological guidelines to maximize the productivity of assembling large steel structures by welding from de-coiled plates with special focus on the guideway assembly for MAGLEV trains are established.

- Before guideway assembly it is necessary to determine;
  - End and eye of the coil
  - Outer and inner surface of the coil
  - Metallurgical description of the material
- Careful heating after de-coiling but before straightening may decrease the residual stress level and provide its uniformity
- Heating after straightening may lead to residual stresses relaxation
- Experimental coefficients  $\delta$  and  $x$  may help to predict the shift of the plate's free end during welding
- Bulging tendency during de-coiling may be calculated from the width to thickness ratio for a given plate
- Based on the general knowledge the tendency for surface cracking is increased with decreasing inner curvature radius
- Temperature-time processing schedule has a great influence on the final plate microstructure and micro-stress level and its distribution



---

## **Meetings and Presentations**

- 3/15/2001 – visit to US Steel to discuss metallurgical aspects of the project
- 3/15/2001 – visit to Maglev Inc. in Monroe, PA to discuss requirements for guideway design and manufacturing
- 4/15/2001 P. Kazanowski, W.Z. Misiolek - Evaluation of Residual in the De-coiling Process, Pittsburg-Monroevill, PA,
- 5/1/2001 – meeting with Air Products Co., Allentown, PA to discuss localized heating technology
- 6/24/2001 P. Kazanowski, W.Z. Misiolek - Evaluation of Residual Stresses and their Influence on Distortion in the De-coiling Process, Office of Naval Research Washington-Carderock, DC
- 8/9/2001 – Follow-up meeting with Air products Co., at Lehigh in Bethlehem
- 11/26/2001 P. Kazanowski, W.Z. Misiolek - Evaluation of Residual Stresses and their Influence on Distortion in the De-coiling and Welding Process, Office of Naval Research Washington-Carderock, DC
- 4/3/2002 P. Kazanowski, W.Z. Misiolek - Evaluation of Residual Stresses and their Influence on Distortion in the De-coiling and Welding Process, Office of Naval Research Washington-Carderock, DC



## References

1. Ashby M.F., **Materials Selection in Mechanical Design**, 2<sup>nd</sup> Ed., Pergamon Press Ltd., (1999), pp. 8-19
2. "Pennsylvania High Speed Maglev Project, Transrapid System Guideway", Overview Pittsburgh 8384 250200, February 25, (2000)
3. Timoshenko S., **Strength of Materials**, D. Van Nostrand Company, Inc., Princeton, NJ, (1956)
4. Hauk V., **Structural and Residual Stress Analysis by Nondestructive Methods. Evaluation – Application – Assessment**, Elsevier, Amsterdam, (1997)
5. Hauk V., **Recent developments in stress analysis by diffraction methods**, Adv. X-ray Anal. 35, (1992), pp. 449-460
6. Kloos E., **Eigenspannungen. Definition und Entstehungsursachen**, Z. Werkestofftech, 10, (1979), pp. 293-332
7. Höller P., Hauk V., Dobmann G. In: Preface to **Nondestructive Characterization of Materials**, eds.: Höller P., Hauk V., Dobmann G, Ruud C.O., Green R.E., Springer – Verlag, Berlin, Heidelberg, (1989)
8. Macherauch E., Wohlfahrt H., Wolfsteig U., **Zur zweckmäßigen Definition von Eigenspannungen**, Härterei – Tech. Mitt., 28, (1973), pp. 201-211
9. Sparing W.H., Radwill R.P., **Stresses in Curved Bars**, Product Engineering, 24, (1962)
10. Shaffer B.W. , House R.N., **The Elastic-Plastic Stress Distribution Within a Wide Curved Bar Subjected to Pure Bending**, Journal of Applied Mechanics, 24, (1955), pp. 305-310
11. Oh S. I., Wu W. T., Tang J. P., Vedhanayagam A., J. Mater. Process. Technol., v. 27, (1991), pp. 25-42
12. Kobayashi S., Oh S. I. Altan T., **Metal Forming and the Finite-Element Method**, Oxford University Press, (1989)

13. Ilegbusi O.J., Iguchi M., Wahnsiedler W., **Mathematical and Physical Modelling of Materials Processing Operations**, Chapman & Hall / CRC (2000)
14. Meerschaert M.M., **Mathematical Modelling**, Academic Press, Inc. (1993)
15. Totten G., Howes M., Inoue T., **Handbook of Residual Stresses and Deformation of Steel**, ASM International, (2002)
16. Ishibashi T., Shimoda S., **The correlation Between Hardness and Flow Stress**, JSME International Journal, Vol. 31, No. 1, (1988), pp. 117-125
17. Cahoon J.R., Broughton W.H., Kutzak A.R., **The Determination of Yield Strength from Hardness Measurements**, Metallurgical Transactions, Vol. 2, (1971)
18. Sines G., Carlson R., **Hardness Measurements for Determination of Residual Stresses**, ASTM Bulletin, Vol. 180, (1952), pp. 35-37
19. **Hardness Testing Handbook**, by V.E. Lysaght and A. DeBellis, American Chain and Cable Company, (1969), pp. 77-97